Volume 9 No 2 December (2026)

e-ISSN: 2615-3270
p-ISSN: 2615-3599

Eigen Mathematics Journal

Homepage Journal: https://eigen.unram.ac.id/index.php/eigen

Stability and Hopf Bifurcation of a Coastal Bridge Reinforcement Corrosion Model: A Delay Differential Equations (DDEs) Approach

Ahmadi[1*]

[1] *Department of Civil Engineering, Universitas Islam Indonesia, Indonesia*
[*] *Corresponding author: ahmadi@uii.ac.id*

A B S T R A C T

This study develops delay differential equations (DDEs) model based on the SIRS framework to examine corrosion dynamics in the reinforcing steel of coastal bridges. The model includes a time delay in the transition from the recovered class to the susceptible class, representing the period during which repaired reinforcement remains protected before becoming susceptible to corrosion again. The basic reproduction number and equilibrium stability are analyzed to identify the conditions under which corrosion can be controlled or persist. For a positive time delay, the corrosion-free equilibrium has a critical delay value of 24.12. At the corrosion-degraded equilibrium, a Hopf bifurcation may occur when the delay reaches the critical value of 2.241, resulting in oscillations in corrosion dynamics. Numerical simulations are used to illustrate the effect of the time delay on the system's behavior. The results show that the delay associated with post-repair protection can influence corrosion dynamics and should be considered when analyzing the long-term behavior of reinforcement in coastal bridges.

Keywords: Delay Differential Equations (DDEs), Corrosion, Bridge Reinforcement, Hopf Bifurcation

Received : 06-08-2026;
Revised : 24-10-2026;
Accepted : 10-11-2026;
Published : 25-11-2026;

DOI: https://doi.org/10.29303/emj.v9i2.463

This work is licensed under a CC BY-NC-SA 4.0 International license

1. Introduction

Corrosion of reinforcing steel is a major durability concern in reinforced concrete structures. [1] reported that steel surface conditions and local inhomogeneities at the steel–concrete interface can significantly affect corrosion initiation. Previous studies have investigated chloride-induced deterioration from several perspectives. [2] developed a reduced chloride ingress model that maintains accuracy while reducing computational costs for long-term service-life assessment under realistic climate and exposure conditions. [3] investigated the interaction between chloride ions and passive films on metals, providing insights into the mechanisms of localized passive film breakdown. In marine concrete structures, [4] examined corrosion-induced cracking under the combined effects of chloride exposure

and fatigue loading, reporting that higher stress levels intensified corrosion and concrete cracking and accelerated corrosion initiation. [5] developed a dual time-variant chloride diffusion model for assessing the probability of corrosion initiation in marine concrete structures and showed that the maximum phenomenon significantly affects the predicted initiation time. [6] investigated the effects of spatial and temporal variations in chloride diffusion, including fluctuations associated with external loading, on chloride concentration and corrosion initiation. Collectively, these studies address the physical mechanisms, environmental influences, and prediction of corrosion deterioration in reinforced concrete structures.

Delay differential equations (DDEs) provide a mathematical framework for describing dynamical systems in which the current rate of change depends on past states. [7] reviewed mathematical modeling involving delays and discussed related dynamical features, including characteristic values and oscillatory solutions. [8] investigated linearized stability analysis for nonlinear delay differential equations with impulses. In epidemiological modeling, examined stability switches in an SIRS model with discrete and distributed delays, whereas [9] analyzed the stability of an SIR model with distributed delays on complex networks. [10] investigated multistability and codimension-two bifurcations in an SIRS-type model with two delays. These studies illustrate how DDEs can be used to investigate delay-dependent stability and complex dynamical behavior. However, the relevance of these analytical approaches to corrosion modeling must be established by considering the specific state variables, transition mechanisms, and parameter interpretations of the corrosion system.

In our previous study [11], we developed an SIRS-based model incorporating a Holling type III function to describe corrosion propagation among reinforcement states in coastal bridge structures. That study analyzed the equilibrium points, local stability, and basic reproduction number without explicitly incorporating a time-delay term. The effect of an explicit delay on the stability properties of that corrosion model was not examined. This limitation motivates the present study, which extends the previous framework by incorporating a time delay into the model.

The present study determines the equilibrium points and their feasibility conditions, analyzes local stability, and examines the characteristic equation as a function of the delay parameter. Particular attention is given to determining whether a critical delay exists at which equilibrium stability changes and Hopf bifurcation occurs. The main contribution is to investigate how an explicit time delay affects the stability properties of the SIRS-type corrosion model and to establish the mathematical conditions under which delay-induced oscillatory dynamics can arise.

2. Research Methods

This study employs mathematical modeling and numerical simulations, to examine reinforcement corrosion in coastal bridges and the effect of delay time on system behavior. A delay differential equations (DDEs) model is developed to represent the interaction between corrosion-free reinforcement, damaged reinforcement, and reinforcement under repair, with delay time capturing the lag in protection and rehabilitation. The model parameters are selected through a trial-and-error approach to obtain plausible system behavior of the proposed model and the qualitative characteristics of reinforcement corrosion in coastal environments. The equilibrium points and basic reproduction number (R_0) are then determined to evaluate whether corrosion will escalate or remain controlled, followed by a stability analysis to assess how small disturbances and changes in delay time influence system dynamics. Furthermore, numerical simulations for several time delay values ($\bar{\tau}$) are carried out using Python to simulate behavior of system, oscillation, and convergence to stability. The final analysis interprets the physical meaning of stability, the basic reproduction number, and time-delay behavior.

3. Result and Discussion

This research is an extension of the study previously published by [11]. The study discusses a corrosion propagation model for coastal bridges without considering time delay. The corrosion process in coastal bridges can be represented using an SIRS (Susceptible-Infected-Recovered-Susceptible) model, in which the different classes represent the stages of corrosion propagation and recovery of the reinforcing steel. The delay differential equation system approach is an interesting modeling framework because the current state of the system depends on its past behavior. Many real-world scenarios involve such events, including the spread of corrosion on the reinforcing steel of a bridge located in a coastal area. This corrosion is caused, in part, by chloride salts (Figure 1). Unlike the ODE-based model in [11], the present study incorporates a time delay in the transition from the recovered class (R) back to the susceptible class (S). This delay reflects the possibility that the recovery of reinforcing steel from corrosion-related effects may not be permanent, and that the steel may become susceptible to corrosion again after a certain period. Therefore, incorporating a time delay provides a more flexible framework for representing the temporal dynamics of corrosion in coastal bridges.

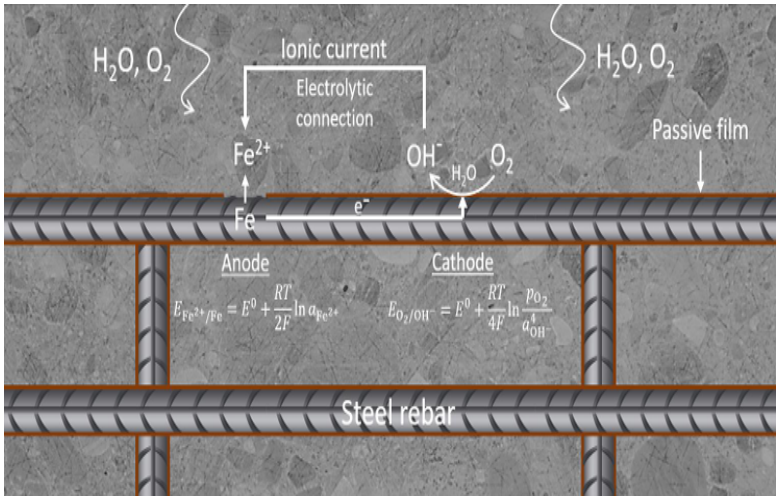

Figure 1. Electrochemical mechanism and localized corrosion areas of reinforcing steel in concrete due to chloride attack (Cl^-) [1]

Chloride ions penetrate the concrete and reach the reinforcement, causing localized corrosion that may gradually spread to the surrounding areas. This process can lead to small cracks in the concrete, which may subsequently provide pathways for further crack propagation. Following the repair of damaged reinforcement, the protective measures introduced during the repair may not lose their effectiveness immediately. Instead, a resistance period may occur before the reinforcement becomes susceptible to corrosion again. In the proposed SIRS model, this period is represented by a time delay, denoted by τ, between the completion of the repair and the transition from the recovered class back to the susceptible class. Thus, reinforcement repaired τ years earlier may begin to lose its protection and become susceptible to corrosion again. Furthermore, corrosion does not develop uniformly across all exposed reinforcement, as the susceptibility to corrosion may vary spatially and temporally. At high chloride-ion concentrations, the corrosion rate may not increase proportionally because of diffusion limitations and changes in surface reaction kinetics. In this study, the Holling type III function is adopted as a phenomenological modeling approach to represent the nonlinear response and saturation effect of the corrosion propagation rate with respect to $S(T)$, the area of reinforcing steel that has

not yet undergone corrosion. This function does not directly represent chloride-ion concentration saturation but serves as a mathematical assumption to capture the qualitative dynamics of corrosion propagation.

$$f(S(T) = \frac{\beta_0 (S(T))^2 I(T)}{1 + \bar{\alpha}(S(T))^2}.$$

Furthermore, with these facts, we constructed delay differential equation system (DDEs).

$$\begin{cases} \frac{dS(T)}{dt} = \mu N(T) - \frac{\beta_0 (S(T))^2 I(T)}{1+\bar{\alpha}(S(T))^2} - \mu S(T) + \xi R(T-\tau) \\ \frac{dI(T)}{dt} = \frac{\beta_0 (S(T))^2 I(T)}{1+\bar{\alpha}(S(T))^2} - (\gamma + \mu) I(T) \\ \frac{dR(T)}{dt} = \gamma I(T) - \mu R(T) - \xi R(T-\tau) \end{cases} \tag{1}$$

with the following table of variables and parameters.

Table 1. Variables and Parameters

Notation	Description	Condition	Units
$S(T)$	The surface area of reinforcement that remains uncorroded at time. This variable represents the portion of the reinforcement surface that has not yet been affected by corrosion and may change over time as corrosion progresses.	$S(T) \geq 0$	area unit
$I(T)$	The surface area of the spread of corrosion on reinforcement that has begun to rust (finely rough) changes over time, visually rust will appear on the surface of the bridge reinforcement.	$I(T) \geq 0$	area unit
$R(T)$	The surface area of corrosion spread of repaired reinforcement (repainting, CFRP (Carbon Fiber Reinforced Polymer) reinforcement) changes over time.	$R(T) \geq 0$	area unit
μ	he rate of natural degradation or replacement of components. For example, the rate of replacement of structures due to service life or natural deterioration.	$\mu \geq 0$	time unit^{-1}
β_0	The rate of corrosion spread from corroded steel to healthy steel. This can occur, for example, due to the diffusion of chloride ions or galvanic contact between metal parts.	$\beta_0 \geq 0$	area unit^{-1} × time unit^{-1}
$\bar{\alpha}$	The chloride diffusion saturation effect, or the limit on the ability of corrosive ions to penetrate concrete, can slow the corrosion rate as more of the metal's surface becomes saturated with ions or the reaction slows down.	$\bar{\alpha} \geq 0$	time unit^{-1}
γ	The rate of structural rehabilitation. The larger γ, the faster the corroded part is repaired.	$\gamma \geq 0$	time unit^{-1}
ξ	The rate of decline in protective effect.	$\xi \geq 0$	time unit^{-1}
τ	Protection duration. For example, an epoxy coating can last up to 10 years before cracking or deteriorating due to exposure to sea air.	$\tau \geq 0$	time unit

System (1) is a system that involves many parameters, so to make it easier to carry out analysis, simplification is carried out. This process is called non-dimensional, take

$$N(T) = S(T) + I(T) + R(T), s(t) = \frac{S(T)}{N(T)}, k(t) = \frac{I(T)}{N(T)}, r(t) = \frac{R(T)}{N(T)}, t = \gamma T \rightarrow \frac{d(\cdot)}{dT} = \gamma \frac{d(\cdot)}{dt}$$

and

$$\bar{\tau} = \gamma\tau, \quad \beta_1 = \beta_0 (N(T))^2, \quad \alpha = \bar{\alpha}(N(T))^2, \quad \beta = \frac{\beta_1}{\gamma}, \quad m = \frac{\mu}{\gamma}, \quad \rho = \frac{\xi}{\gamma}.$$

So, System (1) becomes

$$\begin{cases} \frac{ds(t)}{dt} = m - \frac{\beta(s(t))^2 k(t)}{1+\alpha(s(t))^2} - ms(t) + \rho r(t-\bar{\tau}) \\ \frac{dk(t)}{dt} = \frac{\beta(s(t))^2 k(t)}{1+\alpha(s(t))^2} - (1+m)k(t) \\ \frac{dr(t)}{dt} = k(t) - mr(t) - \rho r(t-\bar{\tau}) \end{cases} \tag{2}$$

with $0 \leq s(t), k(t), r(t) \leq 1$ and initial condition are

$$s(\theta_1) = \varphi_1(\theta_1), \quad k(\theta_2) = \varphi_2(\theta_2), \quad r(\theta_3) = \varphi_3(\theta_3), \quad (\varphi_1(\theta_1), \varphi_2(\theta_2), \varphi_3(\theta_3)) \in C\left([-\bar{\tau}, 0], \mathbb{R}^3_+\right).$$

Furthermore, System (2) is looking for an equilibrium point, this point occurs when the value of the system does not depend on time [12],[13]. So, we have

$$\begin{cases} 0 = m - \frac{\beta(s^*)^2 k^*}{1+\alpha(s^*)^2} - ms^* + \rho r^* \\ 0 = \frac{\beta(s^*)^2 k^*}{1+\alpha(s^*)^2} - (1+m)k^* \\ 0 = k^* - mr^* - \rho r^* \end{cases} . \tag{3}$$

Next, System (3) will be further described in terms of its equilibrium points as follows.

3.1. Equilibrium Point

If System (3) is solved there are two solutions, such solutions are called corrosion-free equilibrium points and corrosion-degraded equilibrium points. This is explained as follows.

3.1.1. Corrosion - Free Equilibrium Point

This equilibrium point will occur when the value of the proportion of the reinforcement class that experiences corrosion will be zero. In other words, the value of $k^* = 0$, so System (3) becomes

$$\begin{cases} 0 = m - ms^* + \rho r^* \\ 0 = -mr^* - \rho r^* \end{cases} \tag{4}$$

and solution of System (4) is $E_1 = (s_1^*, k_1^*, r_1^*) = (1, 0, 0)$. This value indicates that all of the bridge's reinforcing elements in the coastal area have not yet corroded. In other words, none of the bridge's reinforcing elements are actively corroding and do not require repair. This is likely due to the bridge's recent construction.

3.1.2. Corrosion - Degraded Equilibrium Point

The degraded equilibrium point is a condition where some elements have undergone corrosion/damage and remain stable. Based on the third equation of System (3) we get

$$k^* - (\rho + m)r^* = 0 \leftrightarrow k^* = (\rho + m)r^* \tag{5}$$

and the second equation of System (3) can be written as

$$k^* = 0 \quad or \quad \frac{\beta(s^*)^2}{1+\alpha(s^*)^2} - (1+m) = 0.$$

So, we get

$$\frac{\beta(s^*)^2}{1+\alpha(s^*)^2} - (1+m) = 0 \leftrightarrow (s^*)^2 = \frac{1+m}{\beta - (1+m)\alpha}.$$

Since the value of $0 \leq s^* \leq 1$, the value that satisfies the condition is

$$s^* = \sqrt{\frac{1+m}{\beta-(1+m)\alpha}}, \quad with \ \ \beta > (1+m)(1+\alpha). \tag{6}$$

If Eq.(5) and Eq.(6) are substituted into the first equation of System (3), then we obtain

$$r^* = \frac{m(s^*-1)}{\rho} + \frac{\beta(s^*)^2(\rho+m)r^*}{\rho\left(1+\alpha(s^*)^2\right)} \leftrightarrow r^* = \frac{m\rho\,(s^*-1)\left(1+\alpha(s^*)^2\right)}{\rho\left[\rho\left(1+\alpha(s^*)^2\right)-\beta(s^*)^2\,(\rho+m)\right]}.$$

Based on these calculations, we obtain the degraded equilibrium point $E_2 = (s_2^*, k_2^*, r_2^*) = (s^*, k^*, r^*)$ with

$$\begin{aligned} s^* &= \sqrt{\frac{1+m}{\beta-(1+m)\alpha}}, \quad with \ \ \beta > (1+m)(1+\alpha), \\ k^* &= (m+\rho)r^*, \\ r^* &= \frac{m\rho\,(s^*-1)\left(1+\alpha(s^*)^2\right)}{\rho\left[\rho\left(1+\alpha(s^*)^2\right)-\beta(s^*)^2\,(\rho+m)\right]}. \end{aligned} \tag{7}$$

The next step involves determining the basic reproduction number, which is used to assess the extent of the spread of corrosion.

3.2. Basic Reproduction Number of Corrosion

The basic reproduction number is a condition for analyzing the extent to which a corroded area can cause new corroded areas around it. Furthermore, the variable that influences the increase and decrease in corrosion on bridge reinforcement is the variable $k(t)$, which is written as follows [14], [15] .

$$\frac{dk(t)}{dt} = \frac{\beta(s(t))^2 k(t)}{1+\alpha(s(t))^2} - (1+m)k(t).$$

The components that cause increased corrosion are

$$F = \frac{\beta(s(t))^2 k(t)}{1+\alpha(s(t))^2} \rightarrow F(E_1) = \frac{dF}{dk(t)} = \frac{\beta}{1+\alpha}$$

and the components that cause reduced corrosion are

$$M = (1+m)k(t) \rightarrow H\,(E_1) = \frac{dM}{dk(t)} = 1+m.$$

So, the basic reproduction number is obtained $R_0 = FH^{-1} = \frac{\beta}{(1+\alpha)(1+m)}$.
When the value of $R_0 < 1$, the system will move towards a corrosion-free equilibrium point. However, when the value of $R_0 > 1$, the system will move towards a degraded equilibrium point. In the context of corrosion dynamics in bridge reinforcement within coastal regions, the value of R_0 can be interpreted as a threshold parameter that characterizes the potential for corrosion development within the model. When $R_0 < 1$, corrosion-related issues tend to diminish, whereas when $R_0 > 1$, it indicates the potential for corrosion to persist or intensify.
The next step is to determine the stability neighborhood of equilibrium point.

3.3. Local Stability

The motivation for local stability analysis is to analyze the behavior of the system. Because the System (2) is a system of nonlinear differential equations with delays, determining the solution analytically is not possible. Another way to understand the behavior of the system is to analyze the behavior of the system around the equilibrium point. This process is carried out by transforming the equilibrium point to the origin $O(0,0,0)$ using a Taylor series that considers the first order, this process is called Taylor series linearization [12], [16]. Take

$$u(t) = s(t) - s^*, \quad v(t) = k(t) - k^*, \quad w(t) = r(t) - r^*.$$

Hence, System (2) becomes

$$\begin{pmatrix} \frac{du(t)}{dt} & \frac{dv(t)}{dt} & \frac{dw(t)}{dt} \end{pmatrix}^T = A_1 \begin{pmatrix} u(t) & v(t) & w(t) \end{pmatrix}^T + A_2 \begin{pmatrix} u(t-\bar{\tau}) & v(t-\bar{\tau}) & w(t-\bar{\tau}) \end{pmatrix}^T \tag{8}$$

with

$$A_1 = \begin{pmatrix} -a_2 & -a_3 & 0 \\ a_1 & a_4 & 0 \\ 0 & 1 & -m \end{pmatrix}, \quad A_2 = \begin{pmatrix} 0 & 0 & \rho \\ 0 & 0 & 0 \\ 0 & 0 & -\rho \end{pmatrix}$$

and

$$a_1 = \frac{2\beta s^* k^*}{\left(1+\alpha(s^*)^2\right)^2}, \quad a_2 = a_1 + m, \quad a_3 = \frac{\beta(s^*)^2}{\left(1+\alpha(s^*)^2\right)^2}, \quad a_4 = a_3 - (1+m).$$

Let the solution to Eq.(8) be $u(t) = c_1 e^{\lambda\bar{\tau}}, v(t) = c_2 e^{\lambda\bar{\tau}}, w(t) = c_3 e^{\lambda\bar{\tau}}$. Thus, the determinant of the characteristic matrix in Eq.(8) yields the following characteristic equation

$$\begin{aligned} \left|\lambda I - \left(A_1 + A_2 e^{-\lambda\bar{\tau}}\right)\right| &= 0 \\ \begin{vmatrix} \lambda + a_2 & a_3 & -\rho e^{-\lambda\bar{\tau}} \\ -a_1 & \lambda - a_4 & 0 \\ 0 & -1 & \lambda + m + \rho e^{-\lambda\bar{\tau}} \end{vmatrix} &= 0 \\ (\lambda + a_2)\begin{vmatrix} \lambda - a_4 & 0 \\ -1 & \lambda + m + \rho e^{-\lambda\bar{\tau}} \end{vmatrix} + a_1 \begin{vmatrix} a_3 & -\rho e^{-\lambda\bar{\tau}} \\ -1 & \lambda + m + \rho e^{-\lambda\bar{\tau}} \end{vmatrix} &= 0. \end{aligned} \tag{9}$$

Next, the local stability of Eq.(9) is analyzed for the corrosion-free equilibrium point and the corrosion-degradation equilibrium point, as follows.

3.3.1. Corrosion Free Equilibrium Point

If Eq.(9) is examined in the vicinity of the corrosion-free equilibrium point E_1, the result is

$$\begin{aligned} (\lambda + m)\begin{vmatrix} \lambda + (1+m) & 0 \\ -1 & \lambda + m + \rho e^{-\lambda\bar{\tau}} \end{vmatrix} &= 0 \\ p_1(\lambda, \bar{\tau}) \equiv (\lambda + m)\left(\lambda + (1+m)\right)\left(\lambda + m + \rho e^{-\lambda\bar{\tau}}\right) &= 0. \end{aligned} \tag{10}$$

- **Case 1.** When $\bar{\tau} = 0$, the Eq.(10) become

$$(\lambda + m)\left(\lambda + (1+m)\right)(\lambda + m) = 0$$
$$\lambda_1 = -m \quad or \quad \lambda_2 = -(1+m) \quad or \ \lambda_3 = -(m+\rho).$$

  Since $m > 0$ and $\rho > 0$, so all real part ($\mathrm{Re}\{\lambda_i\} < 0, i = 1,2,3$) of characteristic roots are negative. Therefore, the equilibrium E_1 and $R_0 < 1$ is locally asymptotically stable.

- **Case 2.** When $\bar{\tau} > 0$, so the base on Eq.(10), we can state that the real parts of the first two roots, namely $\lambda_1 = -m$ and $\lambda_2 = -(1+m)$ remain negative. Thus, the local stability of E_1 is determined by the roots of the equation $\lambda + m + \rho e^{-\lambda\bar{\tau}} = 0$. To determine its stability in this part, follow the research that has been carried out by [13] . Take $\lambda = i\omega, \omega \in \mathbb{R}^+$, so we get

$$\begin{aligned} (i\omega) + m + \rho e^{-i\omega\bar{\tau}} &= 0 \\ i\omega + m + \rho\left(\cos(\omega\bar{\tau}) - i\sin(\omega\bar{\tau})\right) &= 0. \end{aligned} \tag{11}$$

  Next, we separate the real and imaginary parts, which gives us

$$\omega = \sqrt{(\rho - m)(\rho + m)} \quad with \;\; \rho > m.$$

  The condition $\rho > m$ indicates the possibility of purely imaginary roots. However, this condition alone does not prove that the equilibrium point is unstable. We still need to determine the critical value of the time delay. The real part of Eq.(11) is

$$\cos(\omega\bar{\tau}) = -\frac{m}{\rho}.$$

  Since $\omega > 0$, the imaginary part of Eq.(11) is

$$\sin(\omega\bar{\tau}) = \frac{\omega}{\rho} > 0.$$

  Thus, the critical value of the delay is

$$\bar{\tau}_{01}^{k} = \frac{1}{\sqrt{(\rho - m)(\rho + m)}}\left(\arccos\left(-\frac{m}{\rho}\right) + 2k\pi\right), \quad k = 0, 1, 2, 3, \ldots$$

  For the value of $\rho > m$, we get

$$\bar{\tau}_{01} = \frac{1}{\sqrt{(\rho - m)(\rho + m)}}\left(\arccos\left(-\frac{m}{\rho}\right)\right) > 0.$$

  Hence, if $\rho > m$ and $R_0 < 1$, the equilibrium E_1 is locally asymptotically stable for $0 \le \bar{\tau} < \bar{\tau}_{01}$ and becomes unstable for $\bar{\tau} > \bar{\tau}_{01}$(and $R_0 > 1$). At $\bar{\tau} = \bar{\tau}_{01}$, a pair of characteristic roots lies on the imaginary axis, and the linearized system alone does not establish asymptotic stability. Conversely, if $\rho \le m$, all characteristic roots have negative real parts for every $\bar{\tau} \ge 0$, and E_1 remains locally asymptotically stable.

3.3.2. Corrosion Degraded Equilibrium Point

If Eq.(9) is examined in neighborhood of the corrosion degraded equilibrium point E_2, the characteristic equation derived from Eq.(9) is

$$p_2(\lambda, \bar{\tau}) \equiv \left(\lambda^3 + b_1\lambda^2 + b_2\lambda + b_3\right) + \left(m\lambda^2 + b_4\lambda + b_5\right)e^{-\lambda\bar{\tau}} = 0 \tag{12}$$

with

$$\begin{aligned} &b_1 = m + a_2 - a_4, \quad b_2 = m(a_2 - a_4) - a_2a_4 + a_1a_3, \quad b_3 = (a_1a_3 - a_2a_4)m, \\ &b_4 = (a_2 - a_4)\rho, \quad b_5 = (a_1a_3 - a_1 - a_2a_4)\rho. \end{aligned}$$

- **Case 1.** When $\bar{\tau} = 0$, the Eq.(12) become

$$\lambda^3 + (b_1 + m)\lambda^2 + (b_2 + b_4)\lambda + (b_3 + b_5) = 0.$$

Table 2. Routh–Hurwitz Criteria

Coloumn 1	Coloumn 2
1	$b_2 + b_4$
$b_1 + m$	$b_3 + b_5$
$\frac{(b_1+m)(b_2+b_4)-(b_3+b_5)}{b_2+m}$	0
$b_3 + b_5$	–

Based on Table 2, the first element in the first column of the Routh array is positive. Furthermore, for the conditions $b_1 + m$, $\frac{(b_1+m)(b_2+b_4)-(b_3+b_5)}{b_2+m}$, $b_3 + b_5 > 0$ for $m > 0$ and $\rho > 0$ to hold, all elements in the first column are positive. Therefore, by the Routh–Hurwitz criterion, all roots of the characteristic equation have negative real parts, the equilibrium E_2 and $R_0 > 1$ is locally asymptotically stable [16].

- **Case 2.** When $\bar{\tau} > 0$, we determine local stability in neighborhood E_2, take $\lambda = i\omega, \omega \in \mathbb{R}^+$, so the Eq.(12) becomes

$$\left((i\omega)^3 + b_1(i\omega)^2 + b_2(i\omega) + b_3\right) + \left(m(i\omega)^2 + b_4(i\omega) + b_5\right)(\cos(\omega\bar{\tau}) - i\sin(\omega\bar{\tau})) = 0. \tag{13}$$

If we separate the real part and the imaginary part in Eq.(13), then we obtain

$$\begin{cases} b_3 - b_1\omega^2 = \left(m\omega^2 - b_5\right)\cos(\omega\bar{\tau}) - b_4\omega\sin(\omega\bar{\tau}) \\ b_2\omega - \omega^3 = \left(b_5 - m\omega^2\right)\sin(\omega\bar{\tau}) - b_4\omega\cos(\omega\bar{\tau}) \end{cases}. \tag{14}$$

By algebraic manipulation, the System (14) can be solved as

$$\omega^6 + c_1\omega^4 + c_2\omega^2 + c_3 = 0 \tag{15}$$

with

$$c_1 = b_1^2 - 2b_2 - \rho^2, \quad c_2 = b_2^2 - 2b_1b_3 + 2\rho b_5 - b_4^2, \quad c_3 = b_3^2 - b_5^2.$$

Assuming that ω_0 are the roots of Eq.(15), from System (14) we obtain

$$\begin{bmatrix} e_4 & e_3 \\ e_3 & -e_4 \end{bmatrix}\begin{bmatrix} \cos(\omega_0\bar{\tau}_0) \\ \sin(\omega_0\bar{\tau}_0) \end{bmatrix} = \begin{bmatrix} e_1 \\ e_2 \end{bmatrix} \leftrightarrow \cos(\omega_0\bar{\tau}_0) = \frac{e_1e_4 + e_2e_3}{e_3^2 + e_4^2}$$

with

$$e_1 = b_3 - b_1\omega_0^2, \quad e_2 = b_3\omega_0 - \omega_0^3, \quad e_3 = -b_4\omega_0, \quad e_4 = m\omega_0^2 - b_5.$$

Furthermore, we obtain

$$\bar{\tau}_0^k = \frac{1}{\omega_0}\left(\arccos\left(\frac{e_1e_4 + e_2e_3}{e_3^2 + e_4^2}\right) + 2k\pi\right), k = 0, 1, 2, 3, \ldots. \tag{16}$$

Based on Eq.(16), several possible critical values of the time delay $\bar{\tau}_0$ can be obtained. The minimum critical value is selected as follows

$$\bar{\tau}_0^* = \min\left\{\bar{\tau}_0^k\right\}.$$

Next, the transversality condition is examined, this is necessary because a change in the time delay can lead to a shift in the stability of the equilibrium point E_2.

$$\frac{d\left(\mathrm{Re}\left(\lambda\left(\bar{\tau}\right)\right)\right)}{d\bar{\tau}} \neq 0.$$

If Eq.(12) whose value depends on λ and $\bar{\tau}$ is reduced to $\bar{\tau}$, so we get

$$\left(3\lambda^2 + 2b_1\lambda + b_2\right)\frac{d\lambda}{d\bar{\tau}} + \left(2m\lambda + b_4\right)e^{-\lambda\bar{\tau}}\frac{d\lambda}{d\bar{\tau}} + \left(m\lambda^2 + b_4\lambda + b_5\right)e^{-\lambda\bar{\tau}}\left(-\bar{\tau}\frac{d\lambda}{d\bar{\tau}} - \lambda\right) = 0$$

$$\frac{d\lambda}{d\bar{\tau}} = \frac{\left(m\lambda^2 + b_4\lambda + b_5\right)\lambda e^{-\lambda\bar{\tau}}}{\left(3\lambda^2 + 2b_1\lambda + b_2\right) + \left(2m\lambda + b_4 - \bar{\tau}\left(m\lambda^2 + b_4\lambda + b_5\right)\right)}. \tag{17}$$

Suppose $\lambda\left(\bar{\tau}\right) = v\left(\bar{\tau}\right) + i\omega\bar{\tau}$ are the roots of Eq.(17) which satisfies $v\left(\bar{\tau}_0\right) = 0$ and $\omega\left(\bar{\tau}_0\right) = \omega_0$, so Eq.(17) becomes

$$\left.\frac{d\lambda}{d\bar{\tau}}\right|_{\bar{\tau}=\bar{\tau}_0} = \frac{f_1 + if_2}{f_3 + if_4} = \frac{f_1 f_3 - f_2 f_4}{f_3^2 + f_4^2}$$

with

$$\begin{aligned}
f_1 &= \omega_0\left(b_5\sin\left(\omega_0\bar{\tau}_0\right) - b_4\omega_0\cos\left(\omega_0\bar{\tau}_0\right) - m\omega_0^2\sin\left(\omega_0\bar{\tau}_0\right)\right)\\
f_2 &= \omega_0\left(b_5\cos\left(\omega_0\bar{\tau}_0\right) + b_4\omega_0\sin\left(\omega_0\bar{\tau}_0\right) - m\omega_0^2\cos\left(\omega_0\bar{\tau}_0\right)\right)\\
f_3 &= 2m\omega_0\sin\left(\omega_0\bar{\tau}_0\right) + b_4\cos\left(\omega_0\bar{\tau}_0\right) - \bar{\tau}_0\left(b_5 - m\omega_0^2\right)\cos\left(\omega_0\bar{\tau}_0\right) - \bar{\tau}_0 b_4\sin\left(\omega_0\bar{\tau}_0\right)\\
f_4 &= 2m\omega_0\cos\left(\omega_0\bar{\tau}_0\right) - b_4\sin\left(\omega_0\bar{\tau}_0\right) - \bar{\tau}_0\left(b_5 - m\omega_0^2\right)\sin\left(\omega_0\bar{\tau}_0\right) - \bar{\tau}_0 b_4\omega_0\cos\left(\omega_0\bar{\tau}_0\right).
\end{aligned}$$

To establish the main result of this paper, we impose the following assumption

$$\left.\frac{d\lambda}{d\bar{\tau}}\right|_{\bar{\tau}=\bar{\tau}_0} \neq 0. \tag{18}$$

When Eq.(18) is satisfied, the real part of the characteristic root shifts toward the positive real half of the complex plane as the time delay value increases. Since E_2 possesses a critical time delay $\bar{\tau}_0^*$ and satisfies the transversality condition, a stable limit cycle emerges in the neighborhood of the equilibrium point E_2. In other word, if $R_0 > 1$ the endemic equilibirum E_2 is asymtotically stable when $\bar{\tau} = \bar{\tau}_0^* \in [0, \bar{\tau}_0)$, System (2) undergoes Hopf bifurcation at E_2 when $\bar{\tau} = \bar{\tau}_0^*$ [17], [18].

To cross-check the analytical calculations, the next step is to show a numerical simulation.

3.4. Numerical Simulation

In this section, several numerical simulations are carried out to see the behavior of the system and to cross-check the analysis carried out in the previous section.

3.4.1. Basic Reproduction Number

In the simulation setup, the values $\alpha = 0.2$ and $m = 0.05$ were chosen, so that we ge $R_0(\beta) = \frac{\beta}{1.26}$. When described as follows.

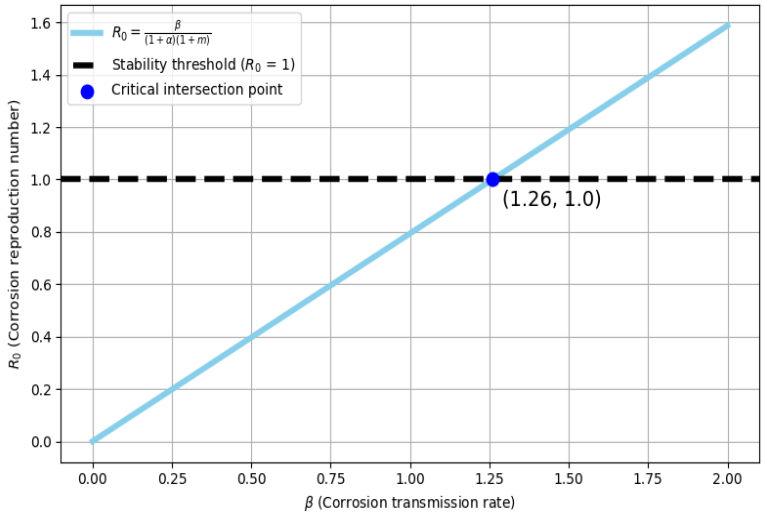

Figure 2. Basic Reproduction Number of Corrosion

Figure 2 illustrates the relationship between the corrosion transmission rate (β) and the basic reproduction number R_0 which serves as a threshold indicator for the potential spread of corrosion in bridge reinforcement. Geometrically, the plot identifies the critical boundary separating parameter associated with different corrosion-spread behaviors. The upward-sloping blue curve indicates that an increase in β leads to an increase in R_0. The horizontal line $R_0 = 1$ represents the critical threshold. The intersection of the two curves defines the critical parameter value $\beta = 1.26$ at which $R_0 = 1$. For parameter values corresponding to $R_0 < 1$, corrosion spread is expected to decline under the conditions established by the model. When $R_0 > 1$, corrosion spread may persist or increase. This threshold interpretation should be distinguished from the stability of the model's equilibrium points, which must be established separately through equilibrium stability analysis.

3.4.2. Corrosion Free Equilibrium Point

In this simulation, the values of $\beta = 0.25, \alpha = 0.2, m = 0.05$ and $\rho = 0.1$ were chosen, as well as the initial values

$$(0.9, 0.1, 0)$$

so that the basic reproduction number is 0.19, and the resulting curve converges to

$$(1, 0, 0).$$

On the other hand, for case $\bar{\tau} = 0$ and we obtain

$$\lambda_1 = -0.05, \ \ or\ \lambda_2 = -1.05, \ \ or\ \lambda_3 = -0.15.$$

Since all the real parts are negative, the system in neighborhood of E_1 will be locally asymptotically stable. Whereas for $0 \leq \bar{\tau} < 24.184$ and the value of $\rho = 0.1 > m = 0.05$ the system in neighborhood at E_1 will be locally asymptotically stable (figure 3).

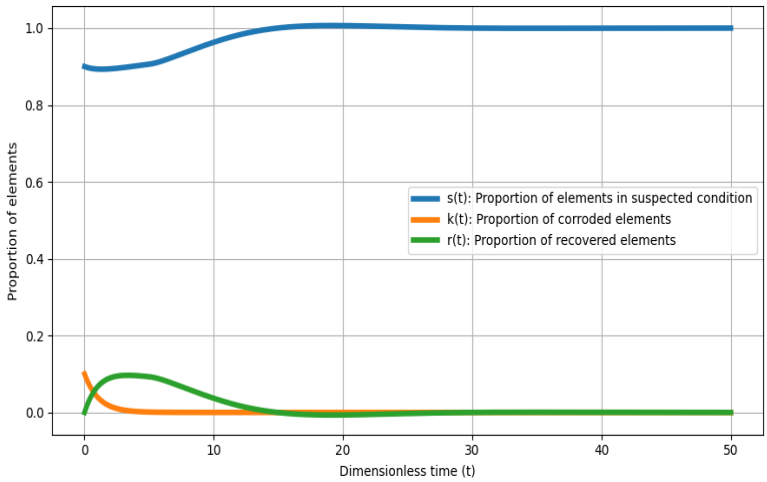

Figure 3. Corrosion-Free Equilibrium Poin

Figure 3 shows how the proportion of bridge reinforcement in good condition gradually increases until it approaches 1, indicating that almost all reinforcement returned to good condition after some time. The orange line shows the proportion of corroded reinforcement. Initially, its value increases, indicating the onset of corrosion, but then decreases to near zero, indicating that corrosion no longer progresses and eventually disappears. Meanwhile, the green line represents the proportion of repaired reinforcement. Its value increases initially, indicating repair, but then decreases as most reinforcement returns to good condition. This graph shows that after an initial increase in corrosion, repair efforts and natural processes in the model cause the reinforcement to stabilize and almost all return to good condition over time.

3.4.3. Corrosion Degraded Equilibrium Point

In this simulation, we choose the following values

$$\beta = 3.5, \alpha = 0.2, m = 0.5, \rho = 1$$

as well as the initial values

$$(0.59, 0.16, 0.25)$$

so that the basic reproduction number was 1.94, and the value of corrosion degraded equilibrium point is $E_2(0.685, 0.189, 0.126)$ and for case $\bar{\tau} = 0$, we obtain

$$\begin{aligned} b_1 + m &= 2.258 > 0, \\ \frac{(b_1 + m)(b_2 + b_4) - (b_3 + b_5)}{b_2 + m} &= 2.352 > 0, \\ b_3 + b_5 &= 1.516 > 0. \end{aligned}$$

Thus, these values satisfy the explanation provided in the previous section (Table 2).

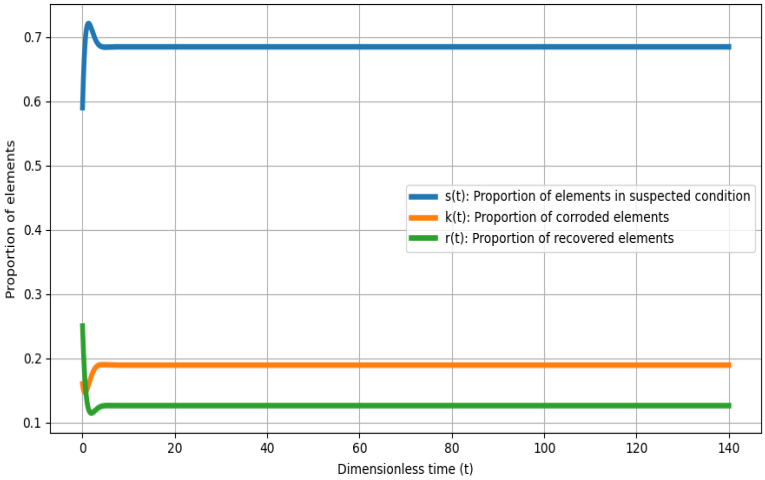

Figure 4. Corrosion- Degraded Equilibrium Point $\bar{\tau} = 0$

Based on the simulation results in Figure 4, the proportions of bridge reinforcement categorized as susceptible to corrosion, actively corroding, or undergoing recovery change quite rapidly during the initial phase before gradually reaching a stable state. In the long term, the proportion of reinforcement susceptible to corrosion is approximately 0.59, the proportion actively corroding is about 0.16, and the proportion undergoing recovery is around 0.25. This indicates that the model, which incorporates a time-delay factor, reaches a stable equilibrium. However, since corrosion persists, the risk of damage to bridge reinforcement in coastal areas remains a significant concern. Furthermore, numerical simulations are performed using the same parameter values as those described previously, yielding the following parameter analysis, delay ($\bar{\tau}$) and simulation results.

$$a_1 = 0.758, \quad a_2 = 1.258, \quad a_3 = 1.50, \quad a_4 = 0, \quad b_1 = 1.758, \quad b_2 = 1.766,$$
$$b_3 = 1.137, \quad b_4 = 1.258, \quad b_5 = 0.379, \quad c_1 = -1.441, \quad c_2 = -1.704,$$
$$c_3 = 1.149, \quad \bar{\tau} = \bar{\tau}_0^* = 2.241, \quad \frac{f_1 f_3 - f_2 f_4}{f_3^2 + f_4^2} = 0.041166 \neq 0.$$

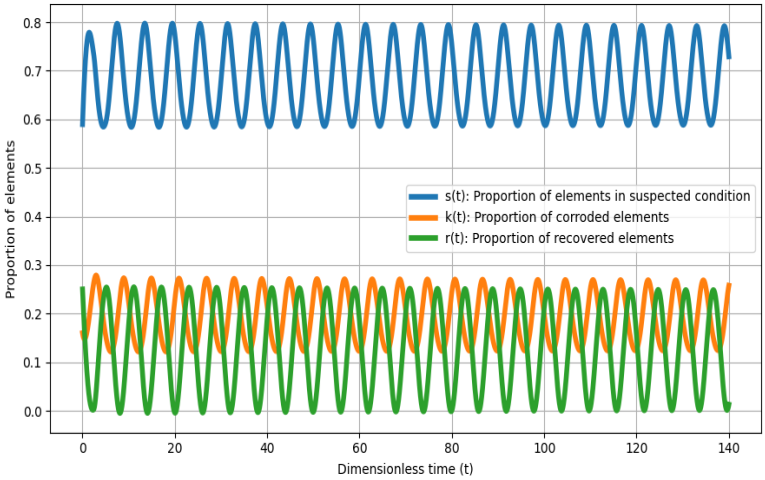

Figure 5. Corrosion- Degraded Equilibrium Point with $\bar{\tau} = \bar{\tau}_0^* = 2.241$

Based on simulation results (figure 5) with a time delay of $\bar{\tau}_0^* = 2.241$, the proportions of reinforcement categorized as susceptible to corrosion, actively corroding, and in a recovery phase exhibit a recurring oscillatory pattern. The proportion of susceptible reinforcement fluctuates between approximately 0.59 and 0.80, the proportion of actively corroding reinforcement ranges from about 0.12 to 0.28 and the proportion of reinforcement in the recovery phase varies between 0 and 0.26. This indicates that the time delay influences corrosion dynamics, preventing the system from reaching a constant equilibrium state and instead causing it to undergo continuous fluctuations.

3.4.4. Behaviors of Time Delay

In this simulation, the values of $\beta = 3.5, \alpha = 0.2, m = 0.5, \rho = 1$ were chosen, as well as the initial values $(0.59, 0.16, 0.25)$ with several delay values.

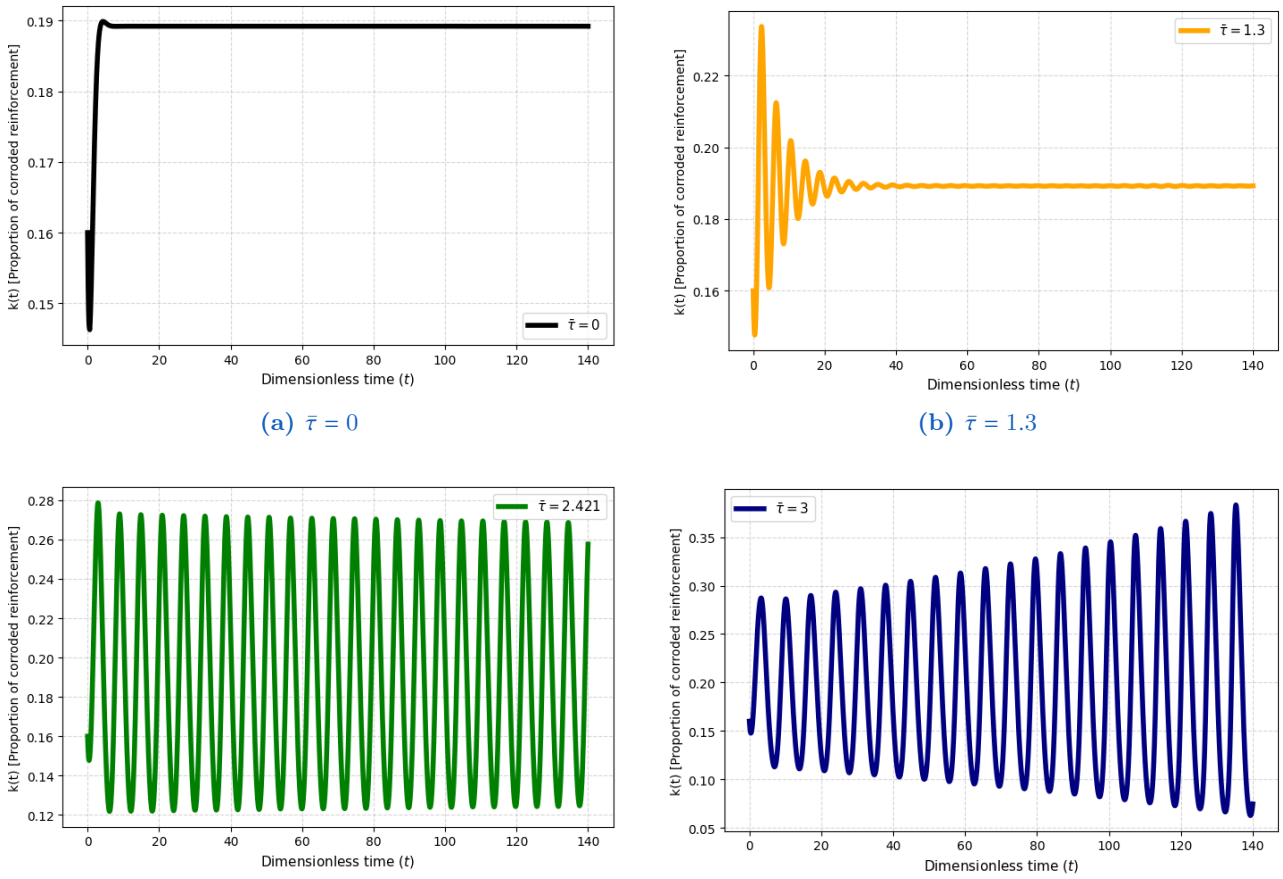

(a) $\bar{\tau} = 0$ **(b)** $\bar{\tau} = 1.3$

(c) $\bar{\tau} = \bar{\tau}_0^* = 2.421$ **(d)** $\bar{\tau} = 3$

Figure 6. Behaviors of Time Delay

Figure 6 illustrates four scenarios regarding the evolution of corrosion levels in bridge steel reinforcement over time, based on variations in the time delay ($\bar{\tau}$), the interval between the ingress of environmental factors (such as coastal salts) and the onset of active corrosion. In figure 6a, where there is no time delay ($\bar{\tau} = 0$), the corrosion level dips slightly at the outset before rising and stabilizing consistently at approximately 0.189. This indicates that, in the absence of a time delay, the extent of damage to the bridge reaches a predictable and stable state relatively quickly. When a short time delay is introduced ($\bar{\tau} = 1.3$), as shown in figure 6b, the corrosion level does not stabilize immediately,

instead, it exhibits initial fluctuations rising and falling over time. Notwithstanding, these oscillations gradually subside, and the values eventually level off toward the same point of stability observed in figure 6a. When the time delay reaches a critical threshold $\bar{\tau}_0^* = 2.241$, as seen in figure 6c, the corrosion level continues to oscillate, forming a recurring, cyclical pattern that fluctuates between 0.12 and 0.27. This suggests that the bridge begins to experience regular, repetitive cycles of damage. On figure 6d, where the time delay extends beyond the safe limit ($\bar{\tau} = 3$), the corrosion system becomes unstable. The amplitude of the corrosion oscillations grows over time, with the peaks continuing to rise. This indicates that longer time delays pose a high risk, potentially leading to extensive and escalating damage to the bridge.

4. Conclusions

This study shows that corrosion dynamics in coastal bridge reinforcement are governed by the corrosion transmission rate and the time delay associated with the corrosion–recovery process. The basic reproduction number, R_0 provides a threshold for distinguishing conditions under which corrosion tends to decline $R_0 < 1$ from those under which it may persist $R_0 > 1$. However, the long-term behavior of the system also depends on the stability of its equilibrium points and the magnitude of the time delay. The numerical results reveal two distinct dynamic patterns. For certain parameter values, the proportions of susceptible, corroding, and recovering reinforcement converge to a stable equilibrium, with long-term proportions of approximately 0.68, 0.18, and 0.12, respectively. Under other conditions, the system exhibits actively corroding oscillations, with the proportion of corroding reinforcement fluctuating between approximately 0.12 and 0.28. These results indicate that corrosion may persist even when the system approaches a stable equilibrium. In addition, the stability analysis identifies a critical time delay at $\bar{\tau}_0^* = 2.241$ which a Hopf bifurcation may occur at the endemic equilibrium. Beyond this critical value, the system may develop persistent or increasing oscillations, depending on the parameter conditions. Thus, the time delay is not merely a temporal value of the model but a factor that can determine whether corrosion dynamics settle toward equilibrium or undergo recurrent fluctuations. From an engineering perspective, these findings highlight the importance of considering the timing and durability of repair and protection measures in coastal bridge maintenance. A stable corrosion level may still represent an ongoing deterioration risk, while oscillatory behavior may indicate recurring transitions between corrosion and recovery. Nevertheless, validation against field measurements is required before the model can be used to estimate actual corrosion levels or establish maintenance thresholds for specific bridges.

References

[1] R. Rodrigues, S. Gaboreau, J. Gance, I. Ignatiadis, and S. Betelu, "Reinforced concrete structures: A review of corrosion mechanisms and advances in electrical methods for corrosion monitoring," 2021. https://doi.org/10.1016/j.conbuildmat.2020.121240.

[2] P. T. Nguyen, E. Bastidas-Arteaga, O. Amiri, and C. P. El Soueidy, "An efficient chloride ingress model for long-term lifetime assessment of reinforced concrete structures under realistic climate and exposure conditions," *International Journal of Concrete Structures and Materials*, vol. 11, no. 2, pp. 199–213, 2017. https://doi.org/10.1007/s40069-017-0185-8.

[3] B. Zhang, J. Wang, B. Wu, X. W. Guo, Y. J. Wang, D. Chen, Y. C. Zhang, K. Du, E. E. Oguzie, and X. L. Ma, "Unmasking chloride attack on the passive film of metals," *Nature Communications*, vol. 9, no. 1, 2018. https://doi.org/10.1038/s41467-018-04942-x.

[4] X. Wang, P. Huang, Y. Yuan, D. Wang, Y. Yang, and X. Liu, "Chloride diffusion and corrosion assessment in cracked marine concrete bridges using extracted crack morphologies," *Buildings*, vol. 15, no. 17, 2025. https://doi.org/10.3390/buildings15173214.

[5] Y. Leng, Z. H. Lu, C. Q. Li, and Y. G. Zhao, "Time-variant probabilistic assessment of corrosion initiation of marine concrete structures considering maximum phenomenon," *Construction and Building Materials*, vol. 272, 2021. https://doi.org/10.1016/j.conbuildmat.2020.121967.

[6] E. Zacchei and C. G. Nogueira, "2d/3d numerical analyses of corrosion initiation in rc structures accounting fluctuations of chloride ions by external actions," *KSCE Journal of Civil Engineering*, vol. 25, no. 6, pp. 2105–2120, 2021. https://doi.org/10.1007/s12205-021-1242-z.

[7] N. J. Ford, "Mathematical modelling of problems with delay and after-effect," *Applied Numerical Mathematics*, vol. 208, pp. 338–347, 2025. https://doi.org/10.1016/j.apnum.2024.10.007.

[8] M. Bachar, "Linearized stability analysis of nonlinear delay differential equations with impulses," *Axioms*, vol. 13, no. 8, p. 524, 2024. https://doi.org/10.3390/axioms13080524.

[9] C. Huang, J. Cao, F. Wen, and X. Yang, "Stability analysis of sir model with distributed delay on complex networks," *PLoS ONE*, vol. 11, no. 8, 2016. https://doi.org/10.1371/journal.pone.0158813.

[10] T. Das, P. K. Srivastava, and S. Singh, "Multistability switches and codimension-2 bifurcation in an sirs(z) model with two delays," *International Journal of Bifurcation and Chaos*, vol. 33, no. 11, 2023. https://doi.org/10.1142/S0218127423501250.

[11] A. Ahmadi, "Dynamic analysis of the sirs model with a type iii holling function on the corrosion distribution of bridge reinforcement steel in coastal areas," *Jurnal Matematika, Statistika dan Komputasi*, vol. 22, no. 2, pp. 469–485, 2026. https://doi.org/10.20956/j.v22i2.48479.

[12] Ahmadi and Widodo, "Local stability of malware propagation model on network computer with two time delay," in *AIP Conference Proceedings*, vol. 2296, 2020. https://doi.org/10.1063/5.0030321.

[13] M. Adimy, F. Crauste, A. Ivanov, and L. Pujo-Menjouet, "Global stability and periodicity in a delay differential model," *Journal of Mathematical Analysis and Applications*, vol. 561, no. 1, 2026. https://doi.org/10.1016/j.jmaa.2026.130555.

[14] B. Chen-Charpentier, "Sirs epidemic models with delays, partial and temporary immunity and vaccination," *AppliedMath*, vol. 4, no. 2, pp. 666–689, 2024. https://doi.org/10.3390/appliedmath4020036.

[15] H. Hu, X. Yuan, L. Huang, and C. Huang, "Global dynamics of an sirs model with demographics and transfer from infectious to susceptible on heterogeneous networks," *Mathematical Biosciences and Engineering*, vol. 16, no. 5, pp. 5729–5749, 2019. https://doi.org/10.3934/mbe.2019286.

[16] F. Y. Saptaningtyas and A. Ahmadi, "Tinjauan matematis waktu tundaan pada model covid-19 dengan vaksinansi," *PYTHAGORAS Jurnal Pendidikan Matematika*, vol. 17, no. 1, 2022. https://doi.org/10.21831/pythagoras.v17i1.49372.

[17] L. Feng, X. Liao, Q. Han, and H. Li, "Dynamical analysis and control strategies on malware propagation model," *Applied Mathematical Modelling*, vol. 37, no. 16-17, pp. 8225–8236, 2013. https://doi.org/10.1016/j.apm.2013.03.051.

[18] Y. Xue and T. Li, "Stability and hopf bifurcation for a delayed sir epidemic model with logistic growth," *Abstract and Applied Analysis*, vol. 2013, 2013. https://doi.org/10.1155/2013/916130.